

Reactions in the Periodontium to Continuous Antigenic Stimulation in Sensitized Gnotobiotic Rats

B. GUGGENHEIM AND H. E. SCHROEDER

Department of Oral Microbiology and Immunology, and Department of Oral Structural Biology, Dental Institute, University of Zurich, Switzerland

Received for publication April 1974

The purpose of our experiment was to evaluate the destructive potential of a strain of *Actinomyces viscosus* on the periodontium of sensitized rodents, describing the induced lesions on the basis of quantitative cytology. The experimental design comprised in principle the following procedures. Young germfree rats were immunized either by intravenous or intradermal injections with heat-killed cells of *A. viscosus* Ny 1 or sham immunized intradermally with physiological saline. After a period suitable for activation of the humoral and cell-mediated immune systems, Ny 1 was monoassociated in all animals by oral implantation. During the ensuing 42 days the animals were allowed to react against the continuous peripheral oral antigen challenge. Since *A. viscosus* is known as a heavy dental plaque-forming organism, the animals could be expected to develop local immunopathological lesions in the periodontal tissues. These lesions were then studied by quantitative cytology after sampling procedures allowing optimal tissue preservation. The degree of bone loss observed in all treatments was unrelated to the destructive capacity of the infiltrates, suggesting the presence of distinct mechanisms responsible for the activation of osteoclasts and factors interfering with fibroblast activity. Although the cellular composition of the infiltrated tissues was analyzed at the end of the experiment only, distinct stages of the lesions in the different treatments allowed reconstruction of the sequence of events. After an acute inflammatory phase, a classic delayed hypersensitivity reaction developed which was transformed after some time by a large superimposed plasma cell accumulation. The particular but undefined immune status was the significant factor determining the final type of peripheral infiltrative reaction.

A series of experiments has shown that certain types of actinomyces induce periodontal destruction in conventional and gnotobiotic rodents (10, 11, 12, 13, 28; S. S. Socransky et al., Arch. Oral Biol., in press). In these experiments, after classical routes of animal experimentation, the selected animal species (e.g., rats and hamsters) were associated with various microorganisms in order to demonstrate a microbial pathogenic potential. In all of these experiments the main focus was on the association of types of microorganisms and the presence and severity of periodontal destruction. Little emphasis was placed on the mode of destructive activity. On the other hand, a number of other quite remote experiments resulted in conceiving periodontal destruction as a manifestation of hypersensitivity reactions (5, 6, 16, 20, 21, 23, 30).

The purpose of our experiment was: (i) to combine the destructive potential of actinomyces in rodents with presensitization by

different routes against the same strain; and (ii) to describe the induced lesions by application of quantitative cytology in order to test the assumption that different types of pathological responses can be discriminated on the basis of infiltrate compositions.

The experimental design comprised in principle the following procedures. Young germfree rats were immunized either by intravenous or intradermal injections with heat-killed cells of *Actinomyces viscosus* Ny 1 or sham immunized intradermally with physiological saline. After a period suitable for activation of the humoral and cell-mediated immune systems, Ny 1 was monoassociated in all animals by oral implantation. During the ensuing 42 days the animals were allowed to react against the continuous peripheral oral antigen challenge. Since *A. viscosus* is known as a heavy plaque-forming organism and germfree rats frequently experience hair impaction in interdental spaces, the animals could be expected to develop local

immunopathological lesions in the periodontal tissues. These lesions were then studied by quantitative cytology after sampling procedures allowing optimal tissue preservation.

MATERIALS AND METHODS

Animals. Eighteen germfree inbred RIC Sprague-Dawley rats originating from four litters were weaned 20 days after birth and transferred into two experimental plastic isolators (8). The animals were caged in screen-bottom stainless-steel cages without bedding. All rats were fed diet 540 S, a low-fat, high-carbohydrate powdered diet containing 40% sucrose, 15% wheat flour (70% extraction), 32% skim-milk powder, 2% vitamin mineral protein supplement (General Protein, Lederle), and 5% brewer's yeast (Engevita). The diet was supplemented with a vitamin mixture according to Gustafsson's diet D 7 (19) and was sterilized by gamma-irradiation (2.5 Mrad). Autoclaved tap water and diet were available ad libitum. The animals were randomly subdivided to form three treatment groups (A, B, and C) of six rats each. The rats were caged in pairs of identical sex and marked with picric acid. Animals of a particular cage did not always belong to the same treatment. At the beginning of immunization the animals were 20 days old.

Immunizing procedures: antigen preparation.

A. viscosus Ny 1 was originally isolated from an Osborne-Mendel rat and kindly provided by J. S. van der Hoeven, University of Nijmegen. The strain was cultured in screw-capped bottles each containing 100 ml of the dialyzable portion of actinomyces broth (BBL). A 57-g amount was dissolved in 200 ml of sterile water and dialyzed three times against 800 ml of water. The pooled dialysates were concentrated under reduced pressure to 1,000 ml in order to avoid any macromolecules on the cells originating from the substrate. After 36 h of incubation at 37 C, the growth of one bottle was harvested by centrifugation. The microorganisms were washed twice in saline and finally resuspended in 5 ml of saline and autoclaved in a sealed ampoule at 120 C during 20 min. The dry weight of this suspension was 24.15 mg/ml. Portions (0.1 ml) of this preparation were used for intravenous injection per animal.

For intradermal injections the strain was processed as described above, except for being suspended in 2.5 ml of saline mixed with an equal volume of complete Freund adjuvant (Difco). A 0.1-ml amount of this preparation was used for intradermal injections per animal.

Immunization schedule. Animals of group A were sensitized by intravenous injections into a lateral tail vein. Prior to injection, the animals were anesthetized by means of an intramuscular injection of 0.05 ml of Hypnorm (N. V. Philips-Duphar, Amsterdam). The animals received six injections at 2- to 3-day intervals prior to and two injections once weekly after oral implantation of Ny 1.

Animals of group C were immunized by intradermal injections at five different sites of the ventral region of the body. The animals received three injections at weekly intervals prior to and one injection 2

weeks after oral implantation of Ny 1. The sham-immunized animals of group B were treated as those of group C, except that 0.1 ml of saline was used for injection.

Oral implantation of *A. viscosus* Ny 1. Ny 1 was grown in 6-ml portions of actinomyces broth (BBL) in screw-capped bottles. After 36 h of incubation at 37 C, the cells were centrifuged and the supernatant was decanted under laminar air flow. Sediments of six vials each were resuspended in 6 ml of fresh broth and transferred to ampoules which were sealed and passed into the isolators.

All rats were inoculated orally with 0.2 ml of broth per animal once on 3 subsequent days by using a tuberculin syringe. At this point of the experiment the average age of the rats was 41 days.

Microbial controls. Isolators prepared for this experiment were found to be sterile when water, diet, and surroundings were checked. All animals were controlled for contamination before being transferred from the breeding isolators into experimental isolators using an extensive test program (Hurni and Hämerli, unpublished data). No microbial contaminations could be detected. At the end of the experiment, i.e., 42 days after oral implantation, anal and oral swabs of each animal were taken. This material was used to inoculate fluid cultures and plates. Ny 1 was found regularly in oral swabs but only occasionally in feces. After sacrifice, plaque samples from two animals of each treatment were used to inoculate blood plates. Ny 1 was present as the only organism on all plates, which indicated that this strain did not colonize or only weakly colonized in the intestine.

Determination of antibody titers. Peripheral blood was collected prior to the experiment from a small number of surplus animals. At the end of the experimental period, peripheral blood was collected from all animals. The sera was subjected to a microcomplement fixation test (29).

The antigen used for this test was prepared as follows. Strain Ny 1 was cultured in the dialyzed part of actinomyces broth (BBL) at 37 C. After centrifugation the cells were washed three times with saline, resuspended in 5 ml of saline, and sonically treated at maximum power in a Branson B-12 sonicator equipped with a microtip. The sonicate was centrifuged at 20,000 $\times g$ for 15 min. The supernatant served as antigen preparation, the properties of which had been examined in the usual series of pre-experimental tests.

Processing of tissue. Immediately after decapitation, upper and lower jaws of all animals were excised. Upper and lower molars were regularly covered by massive actinomyces plaques as revealed by staining with Erythrosine.

Lower jaws were fixed in 10% buffered formalin, macerated, dried, and used for a standardized evaluation of the distance between the cementoamel junction (CEJ) and the crista alveolaris on the lingual side. For better visualization of the CEJ the jaws were stained with saturated aqueous methylene blue. Upper jaws were prefixed by immersion and decalcified in ethylenediaminetetraacetic acid according to routine procedures (26).

Under a dissecting microscope, the right and left

alveolar portions were dissected and trimmed to form rectangular cubes comprising the three molars and the surrounding soft and hard tissue. These cubes were then subdivided in buccopalatal direction into five blocks. The first block included the anterior part of the first molar (m_1). The second block included the central part of m_1 . The third block contained the interdental space between m_1 and m_2 , including the distal part of m_1 and the mesial part of m_2 . The fourth block included the central part of m_2 . The fifth block comprised the interdental space between m_2 and m_3 , including the distal part of m_2 and the mesial part of m_3 .

Blocks 1, 2, and 4 were further subdivided along the middle axis of the teeth into a palatal and a buccal part. Thereafter all blocks were postfixed in OsO₄ and embedded according to standard procedures (24). Both parts of blocks 1, 2, and 4 were oriented in a buccopalatal plane parallel to the Epon surface. Blocks 3 and 5 were oriented in a mesiodistal plane. From both parts of block 2 and from block 3, two 1- to 2- μ m-thick random sections were cut with the Reichert OM-U2 ultramicrotome by using glass knives, doubly stained with period acid-Schiff stain and toluidine blue (25), and mounted in Permount. From each group four buccal portions of block 2 and four of block 3 (interdental tissue) revealing maximally extended lesions were selected for electron microscopic observation. Ultrasections comprising the entire buccal or interdental gingival tissue, respectively, were prepared by using a diamond knife (DuPont) and the LKB Ultratome I. They were contrasted with uranyl magnesium acetate followed by lead citrate (3, 22). Electron micrographic recordings were obtained

with a Philips 300 electron microscope.

Quantitative evaluation procedures: determination of bone level on macerated lower jaws. All jaws were photographed under standardized conditions by using a Leitz Aristophot and Kodachrome diapositive film. The magnification was adjusted to a level allowing simultaneous reproduction of the lingual side of m_1 and m_2 . The diapositives were subjected to a point-counting procedure. This was done in a table projector unit (31) yielding a final magnification of $\times 55$. The projector screen was equipped with a coherent double-lattice test system comprising 99 heavy and 891 light points (31). A typical diapositive superimposed with the test system is shown in Fig. 1. The axis of test lines was turned to intersect with the general plane of the alveolar bone crest at an angle of approximately 20°. This was done in order to avoid a coincidence of orientation of the alveolar crest with the lines of the test system. All light points superimposed on the root surface between the CEJ and the alveolar bone crest were counted (Fig. 1). The counting was performed separately for m_1 and m_2 . In addition, the distance between the projected margins of the mesial and distal root surfaces was measured by using a ruler with 0.5-mm gradation. Area points were transformed to express the exposed root surface area in square micrometers. The mesial-distal width of m_1 and m_2 was expressed in micrometers. Both data served to calculate the average distance between CEJ and alveolar bone crest per tooth for single jaws as well as for groups of animals.

Histometric measurements on random semithin sections of upper jaws. The distance between the level of the alveolar bone crest and the CEJ as well as

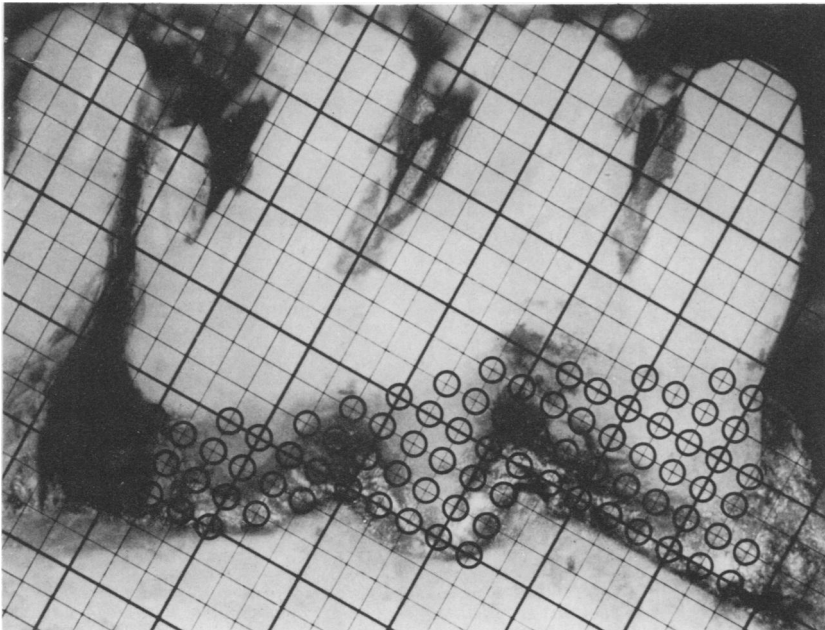


FIG. 1. Lingual view of the first lower rat molar superimposed with a stereological test system. The methylene blue-stained specimen reveals the cemento-enamel junction (faint line), residual collagenous tissue of the periodontal ligament (dark), and the alveolar bone crest. Points falling upon the cementum surface are marked (circles).

between the apical termination of the junctional epithelium (JE) and the CEJ (see Fig. 2) was measured on one random section each from the palatal and buccal parts of block 2 and from block 3 (interdental) of right and left upper jaws of two animals per experimental group. A total of 36 sections was analyzed. Measurements were performed by using a microscope fitted with an ocular micrometer. Average data per group of animals were expressed in micrometers.

Morphometric measurements on random semithin sections of upper jaws. The same series of random sections as used for histometric measurements was subjected to morphometric point-counting procedures. These served for the estimation of the volumetric density of gross tissue components (Fig. 2): epithelium, connective tissue, and the infiltrated connective tissue (ICT) portion. The components were estimated by superimposing a coherent double-lattice test system comprising 25 heavy and 100 light points with the stained section using a Wild sampling microscope M-501 (32). The area comprising the gingival tissue to be analyzed (= sample size) was delineated as shown in Fig. 2a and b. By using the heavy point lattice, a magnification of $\times 400$ and a consecutive field-to-field sampling covering the delineated tissue area, as well as the gross tissue components, were differentially counted.

Morphometric measurements on electron micrographs of ultrathin sections. To quantitatively analyze the ICT composition, a standardized series of nine electron micrographs was recorded from the ICT area only. A multipurpose test system comprising 42

volumetric points (31) and a magnification of $\times 11,400$ was used to estimate the volumetric and numerical densities per ICT unit volume of fibroblasts, neutrophilic granulocytes, monocytes/macrophages, small and medium-sized lymphocytes, immunoblasts, x-lymphocytes (an unidentified cell type), plasma cells, and mast cells, as well as the volumetric density of collagen fibrils. All residual tissue components, such as blood and lymphatic vessels, nerves, interstitial ground substance, and unidentified cell portions, were pooled. The total sample size analyzed per gingival site and treatment group was $14,700 \mu\text{m}^2$ of infiltrated connective tissue.

Details of the procedures used for recording electron micrographs, morphometric point counting, recording and computation of raw data were described previously (27). All resulting data were expressed in cubic millimeters per cubic centimeter of gingival tissue. All numerical density data were expressed per cubic centimeter of ICT.

RESULTS

Upon clinical inspection, upper and lower jaws of all animals showed massive aggregates of actinomyces plaque-forming broad garlands which encircled each molar and crossed the occlusal surface through the fissure spaces. Interdentally as well as on buccal sites, single or bundled groups of hair could frequently be encountered impaled between hard and soft tissue.

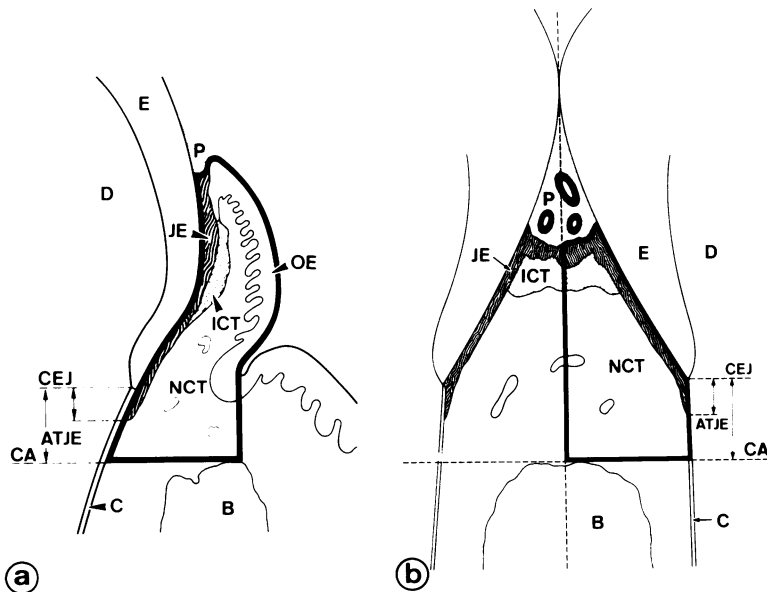


FIG. 2. Schematic drawings illustrating gross structures of buccal (a; linguobuccal cross-section) and interdental (b; mesiodistal cross-section) gingival tissues at upper rat molars. The areas outlined represent the tissue sample used for morphometric analysis. Arrowheaded lines mark distances measured histometrically. Abbreviations: ATJE, Apical termination of JE; B, bone; C, cementum; CA, alveolar bone crest; CEJ, cemento-enamel junction; D, dentin; E, enamel; ICT, infiltrated connective tissue; JE, junctional epithelium; OE, oral epithelium; P, plaque; NCT, noninfiltrated connective tissue.

Antibody titers. Nonsensitized germfree animals revealed insignificant titers. The final titers determined in groups A, B, and C are listed in Table 1. The highest titers were found in intravenously immunized animals of group A. Weak titers were found in the intradermally sensitized animals of group C, whereas the sham-immunized rats of group B showed even lower but still significant titers.

Alveolar bone level. The average distance between the CEJ and the level of the alveolar bone crest at lingual sites of lower first and second molars are compiled in Table 1. For both teeth this distance was significantly greater in animals of group A compared with groups B and/or C. Furthermore, the distance found at the second molar was always markedly smaller than that determined for the first molar.

The histometric measurements estimating the distance between the CEJ and the level of the alveolar bone crest in random sections of buccal and interdental tissue of upper molars did not reveal any group differences. At buccal sites of first molars, this distance was $341 \pm 48 \mu\text{m}$ in group A, $376 \pm 43 \mu\text{m}$ in group B, and $312 \pm 53 \mu\text{m}$ in group C. At the interdental site between m_1 and m_2 , this distance was $460 \pm 121 \mu\text{m}$, $431 \pm 117 \mu\text{m}$, and $555 \pm 79 \mu\text{m}$, respectively (means \pm standard deviation). The distance between the CEJ and the apical termination of the JE at the tooth surface were practically zero in all treatment groups with respect to the buccal site of the first molar. At the interdental site between upper m_1 and m_2 ,

the epithelium had proliferated along the cementum surface in some animals of each group. The distance between CEJ and the apical termination of JE amounted to $48 \pm 70 \mu\text{m}$ in group A, $55 \pm 77 \mu\text{m}$ in group B, and $45 \pm 36 \mu\text{m}$ in group C (means \pm standard deviation).

Histological observations. Sections derived from the buccal and interdental gingival tissue at upper first molars from animals in all three groups revealed the following structural alterations. The marginal gingiva was enlarged in width and frequently distorted in shape (Fig. 3). Dense clusters of actinomyces plaque were located either coronal to the gingival margin or within a pathologically deepened sulcus (Fig. 3c). These clusters were always superficially surrounded mainly by polymorphonuclear leukocytes, which were most numerous in animals of group C (Fig. 4e). Actinomyces cells could not be encountered within the soft tissues. In all instances the coronal portions of the JE were destroyed or lacking. In the region of the CEJ or along the root surface apical to the CEJ, short residual strands of JE were more or less heavily transmigrated or infiltrated by leukocytes (Fig. 3b and d; 4b, d and f). The epithelial attachment to either enamel or cementum was maintained by only a very small number of JE cells (Fig. 3b, d, and f; 4b, d, and f). This had resulted in the formation of pathological deepened sulci or pockets, filled in part with plaque, hair, and leukocytes (Fig. 3 and 4). The infiltrated connective tissue portions resided primarily beneath and along the JE, but extended variably in a lateral and/or apical direction (Fig. 3 and 4). The collagen fiber arrangement was strikingly altered by infiltration and the fiber attachment was strongly impaired in those areas where ICT had spread beyond the CEJ.

In principle, similar observations could be made in gingival tissue sections derived from interdental sites (Fig. 4). The surface of the interdental gingiva was flat and covered by a very thin and occasionally apically proliferating CE (Fig. 4a, c, and e). The interdental space, coronal to the flattened tissue, was more or less densely packed with actinomyces plaque, leukocytes, and hair (Fig. 4a, c, and e). Hair could be observed to reach deep into the soft tissue (Fig. 4a and b). Not infrequently, tangentially sectioned hair portions were surrounded by multinucleated giant cells (Fig. 4b). In general, most apically located hair portions were found to be embedded in an infiltrative cell population of variable size.

The most striking structural feature of both buccal and interdental tissue sites was the different character of the connective tissue

TABLE 1. *Titers of microcomplement fixation tests and level of alveolar bone crest in relation to the cemento-enamel junction in lower jaws at lingual sides of the first (m_1) and the second (m_2) molars of three differently treated groups of rats*

Determination	Treatment group		
	A	B	C
AB titer			
Range	256-1,024	16-64	64-256
Mean	512	32	128
Alveolar bone level ^a			
m_1	785 ± 79^b	647 ± 34	695 ± 70
m_2	$471 \pm 93^{c,d}$	327 ± 36	372 ± 50

^a Data expressed in micromoles.

^b Significantly different from group B value at a 0.01 level.

^c Significantly different from group C value at a 0.05 level; significantly different from group B value at a 0.001 level.

^d Significantly different from group C value at a 0.001 level.

infiltrates. All sections of animals in group A revealed comparatively large infiltrates with plasma cell predominance (Fig. 3b and 4b). These infiltrates were always poor in extravascular neutrophilic granulocytes. On the other hand, all sections of animals of group C exhib-

ited small peripheral infiltrates in which plasma cells could hardly be recognized (Fig. 3f and 4f). Typical for these lesions were the excessive numbers of extravascular granulocytes. Although sections belonging to group A and C could be recognized on the basis of these

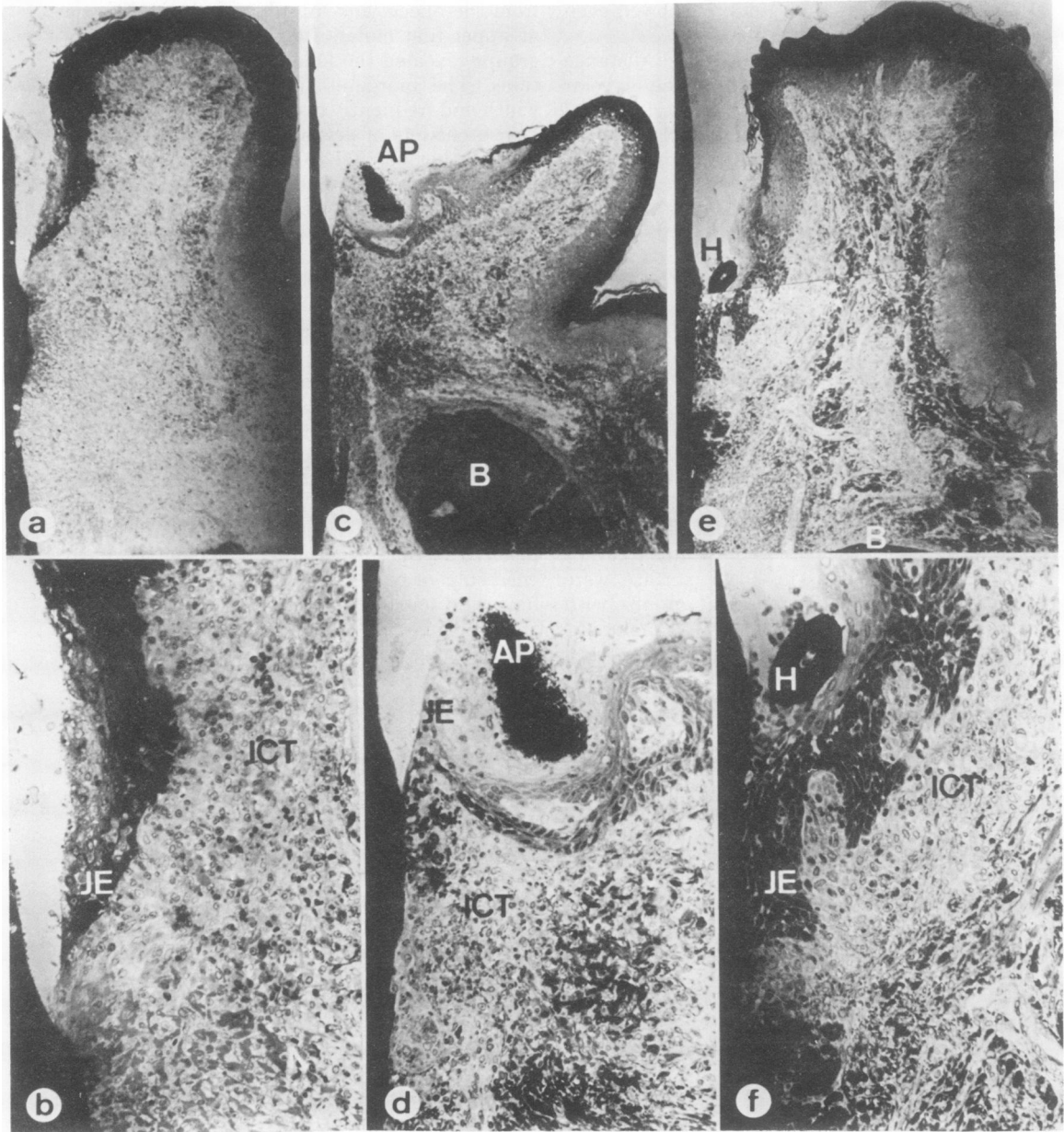


FIG. 3. Pathological alterations of buccal gingival tissue at upper first molars from rats of group A (a, b); B (c, d), and C (e, f) shown at low (a, c, e) and higher (b, d, f) magnification. Actinomyces plaque (AP), hair (H), gingival pockets, the residual junctional epithelium (JE), as well as the infiltrated connective tissue (ICT), are clearly visible. The ICT extends deeper and contains more plasma cells in group A (a, b) than in group C animals (e, f). B, Alveolar bone. Magnification: a, c, e = $\times 130$; b, d, f = $\times 320$.

criteria, those of group B were impossible to separate.

Quantitative stereological characteriza-

tion of tissue infiltrates. The quantitative analysis of infiltrate composition confirmed and supplemented the histological observations.

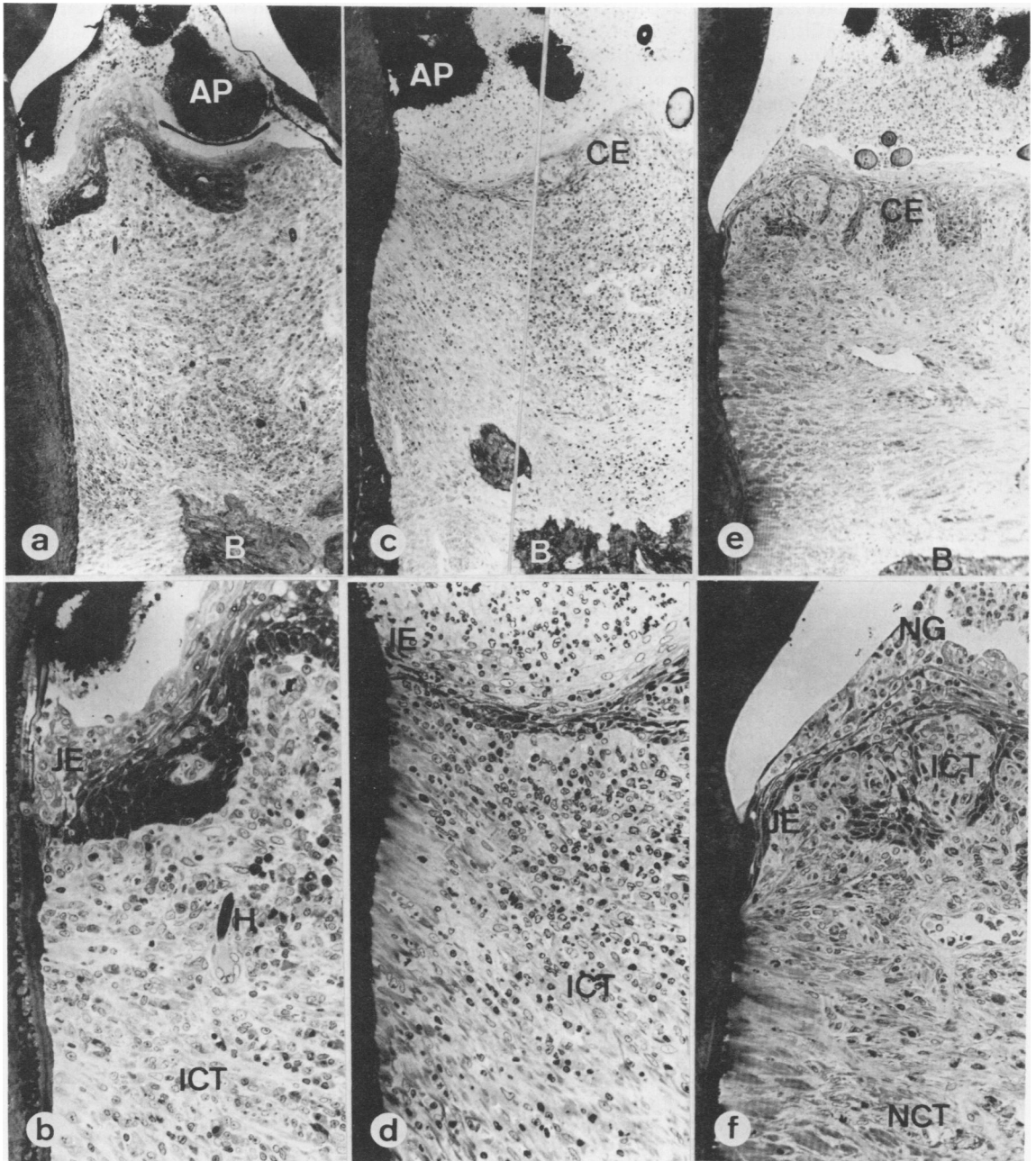


FIG. 4. Pathological alterations of interdental gingival tissues between upper first and second molars of rats of group A (a, b), B (c, d), and C (e, f) shown at low (a, c, e) and higher (b, d, f) magnification. Actinomyces plaque (AP), hair (H), the flat col epithelium (CE), the residual junctional epithelium (JE), and the infiltrated connective tissue (ICT) coronal to the alveolar bone crest (B) can be recognized. Infiltrates of group A (b) and B (d) rats have spread deeply into the trans-septal collagen fiber bundles and contain numerous plasma cells. The infiltrate of group C is small and resides peripherally (e, f). Magnification: a, c, e = $\times 130$; b, d, f = $\times 320$.

Volumetric and numerical density data describing the ICT size and the density and percentage contribution of various cell populations constituting the connective tissue infiltrates are compiled in Tables 2 and 3. With the exception of treatment B infiltrates, there was a remarkable similarity at buccal and interdental sites of animals belonging to the same group.

Buccal gingival tissue. Although both the epithelium and overall connective tissue were of similar size in all groups of animals, the ICT was markedly larger in animals of group A compared with those of groups B and C (Table 2). Percentagewise, collagen fibrils occupied a smaller volume in infiltrates of group A compared with groups B and C. The total cell population amounted to half of the volume of the infiltrates in all groups (Table 2).

The total number of cells present per unit volume of ICT was rather similar for group A ($1,200 \times 10^6$), for group B ($1,800 \times 10^6$), and for group C ($1,400 \times 10^6$). The numerical density of the various cell types, however, was strikingly different between group A and C (Fig. 5).

TABLE 2. Volumetric density parameters characterizing buccal gingival tissue in three differently treated groups of rats^a

Constituent	A ($\bar{x} \pm SD$)	B ($\bar{x} \pm SD$)	C ($\bar{x} \pm SD$)
Gingival tissue	1,000	1,000	1,000
Epithelium	288 ± 46	348 ± 44	338 ± 20
Connective tissue	712 ± 49	652 ± 44	662 ± 20
Infiltrated CT	310 ± 248	144 ± 134	91 ± 23
Collagen fibrils	29 (9)	26 (18)	13 (14)
Cells	161 (52)	79 (55)	39 (43)
Residual tissue	120 (39)	39 (27)	39 (43)

^a $\bar{x} \pm SD$ = Mean and standard deviation; N = 4; percentages of connective tissue components are given in brackets. Parameters were measured as cubic millimeters per cubic centimeter of gingival tissue.

TABLE 3. Volumetric density parameters characterizing interdental gingival tissue in three differently treated groups of rats^a

Constituent	A ($\bar{x} \pm SD$)	B ($\bar{x} \pm SD$)	C ($\bar{x} \pm SD$)
Gingival tissue	1,000	1,000	1,000
Epithelium	116 ± 48	65 ± 45	116 ± 43
Connective tissue	884 ± 48	935 ± 45	884 ± 43
Infiltrated CT	582 ± 245	357 ± 235	178 ± 34
Collagen fibrils	81 (14)	24 (7)	7 (4)
Cells	314 (154)	240 (67)	63 (36)
Residual tissue	187 (32)	93 (26)	108 (60)

^a See Table 1.

Fibroblasts were considerably less numerous in group A (182×10^6) than in group C (533×10^6) infiltrates (Fig. 5). Cells belonging to the lymphocyte series constituted about 80% of group A infiltrates compared with 35% of group C infiltrates (Fig. 6a). Particularly striking was the predominance of plasma cells in group A (321×10^6) and their scarceness in group C (15×10^6) infiltrates. On the other hand, few neutrophilic granulocytes and macrophages were found in group A (32×10^6 and 40×10^6 , respectively) and remarkably numerous in group C (293×10^6 and 95×10^6 , respectively) infiltrates (Fig. 5 and 6). In comparison, the infiltrate composition of group B animals, although including a

$N_V \times 10^6 / \text{cm}^3 \text{ ICT}$

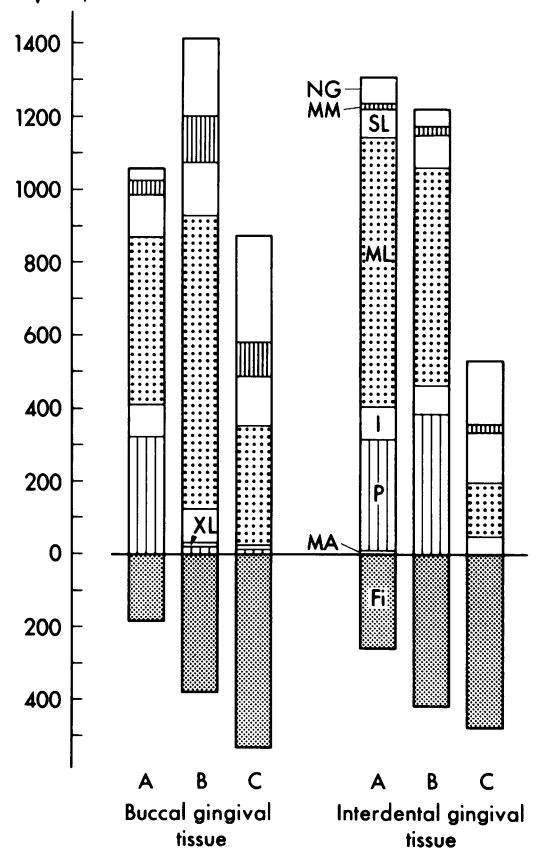


FIG. 5. Numerical density ($N_V \times 10^6 / \text{cm}^3 \text{ ICT}$) of various cell populations constituting the connective tissue infiltrates (ICT) in buccal and interdental gingival tissue at upper molars in three differently treated groups of rats (A, B, C). Fibroblasts (Fi) are separately listed below the 0-line. Abbreviations: NG, Neutrophilic granulocytes; MM, monocytes and macrophages; SL, small lymphocytes; ML, medium-size lymphocytes; I, immunoblasts; XL, unidentified lymphoid cells; P, plasma cells; MA, mast cells.

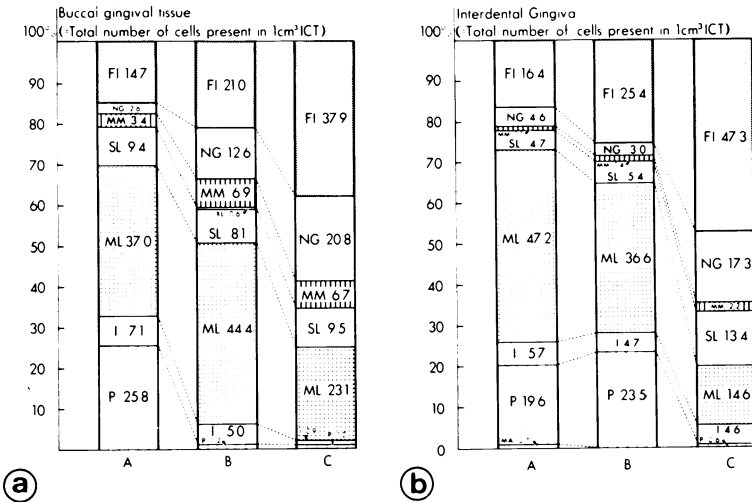


Fig. 6. Percentage of contribution of the various cell populations constituting connective tissue infiltrates (ICT) in buccal (a) and interdental (b) gingival tissue at upper molars in three differently treated groups of rats (A, B, and C).

59% lymphoid cell contribution, impressed by a high number of neutrophilic granulocytes (229×10^6) and macrophages (125×10^6) in connection with very few plasma cells (22×10^6) but an elevated number of immunoblasts (91×10^6 ; Fig. 5 and 6).

Interdental gingival tissue. Most of the striking differences observed for buccal connective tissue infiltrates of group A and C similarly applied to the interdental tissue. ICT size was large in group A and consistently small in group C animals (Table 3). Because the infiltrate in group A animals had deeply spread between the trans-septal collagen fiber bundles located coronal to the interdental bone crest (Fig. 4a), the collagen volume was larger in this group compared to group C (Table 3). The total cell population present constituted more than 50% of the ICT volume in groups A and C, but only 36% in group C (Table 3). The total number of cells present per unit volume of ICT (Fig. 5) was similar in groups A and B ($1,560 \times 10^6$ and $1,640 \times 10^6$, respectively) but markedly lower in group C ($1,000 \times 10^6$). In both groups A and B about 70% of the cells belonged to the lymphocyte series. Immunoblasts (77×10^6 and 89×10^6 , respectively) and plasma cells (307×10^6 and 386×10^6 , respectively) were equally numerous in both groups (Fig. 5 and 6). On the other hand, only 33% lymphoid cells contributed to the group C infiltrates in which plasma cells (6×10^6) were extremely scarce (Fig. 5 and 6). In accordance with the composition of infiltrates at buccal sites, the interdental tissue infiltrates of group C animals impressed by the predominance of neutrophilic

granulocytes (175×10^6) which were less dense in group A and B (72×10^6 and 49×10^6 , respectively) infiltrates. Fibroblasts were less numerous in group A (257×10^6) than in group B (417×10^6) and C (477×10^6) infiltrates (Fig. 5 and 6).

In general, the ICT composition of group A animals was strikingly similar at both buccal and interdental sites. The same degree of similarity was found in both sites of group C animals. Group B animals, however, revealed differences in ICT composition between buccal and interdental tissue which resembled those described for group C and A animals. Although in buccal tissue the ICT composition of group B resembled that of group C, in interdental tissue B infiltrates were similar to A infiltrates.

DISCUSSION

Our data appear to elaborate on the relationship between the mode of sensitization and the type of local reaction which develops in the periodontium on the continuous local antigenic challenge. Animals previously sensitized intravenously (group A) developed and maintained high antibody titers. These animals reacted locally with a large gingival connective tissue infiltrate at both buccal and interdental sites. These infiltrates were predominantly comprised of plasma cells, whereas the acute cellular exudation was rather small. Fibroblasts were markedly reduced in number and collagen fibers in volume. Furthermore, as measured in the lower jaw, a significantly greater bone loss than in group C animals could be established at lingual sites. The individual degree of bone loss

was not correlated with the antibody titer prevailing in the same individual animal. On the other hand, animals previously sensitized intracutaneously (group C) exhibited still significant but markedly lower antibody titers than group A. These animals had reacted with only small peripheral infiltrates on buccal as well as interdental sites. At both sites the infiltrate comprised a lymphocyte predominance, contained a very small number of plasma cells, and was distinguished by the elevated level of acute cellular exudation. The infiltrated connective tissue area revealed a normal numerical fibroblast density. Animals of group B, previously sham immunized and subsequently through continuous presence of actinomyces plaque sensitized and challenged locally, had reacted differently at buccal and interdental sites. Although in the buccal tissue the lesion was similar to that in group C animals, the interdental lesion resembled that of group A animals.

These results were obtained by combining germfree animal experimentation with serological and stereological analysis. For methodological reasons the latter could not be applied equally to upper and lower jaws because (i) both measurements on the defleshed jaws and histometric and stereological analysis could not be performed on the same specimen, and (ii) both methods required a double estimation on right and left quadrants. For these reasons several portions of the overall results were gained from one or the other jaw only. The average distance between the CEJ and the level of alveolar bone crest, estimating the horizontal bone loss, was measured by stereological methods. In comparison with the more simple direct reading of this distance at special reference points as described by Keyes and Gold (14), and with the equally laborious method of tracing and paper weighing as described by Costich (1), the stereological approach had the advantage of being simple in performance and producing more accurate overall averages per tooth which could be expressed in micrometers. The obtained results were incompatible with those gained from histometric measurements of the same distance in random sections of buccal and interdental tissue at the upper first molar. This incompatibility is due to only a small part of the fact that an overall average value cannot be expected to coincide with a randomly measured figure at one particular location. It has been found that the two above-mentioned measurements, although not absolutely similar, can still be shown to correspond in demonstrating a decreasing or increasing trend of the alveolar bone level (Schroeder and Jossi, un-

published data). The major reason for incompatibility of the above-mentioned data is that in a noninfected normal rat the distances between the CEJ and the alveolar bone crest differ markedly between upper and lower jaws at the various sites and furthermore, in part change with age. At the lingual aspect of lower molars, this distance increases steadily in 30- to 80-day-old germfree rats, whereas it remains rather constant at buccal and interdental sites around upper first molars (Schroeder and Jossi, unpublished data). In 80-day-old rats (an age comparable to the 83-day-old animals of the present study) the control distance for lingual sites of lower molars would be $575 \pm 20 \mu\text{m}$ for m_1 and $290 \pm 20 \mu\text{m}$ for m_2 . The control distances at the mesial portion of m_1 in the upper jaw would be $150 \mu\text{m}$ for buccal sites and $100 \mu\text{m}$ for the interdental site between upper m_1 and m_2 . Comparing these control figures with those of the present study it is obvious that both average data for lower molars as well as selective data for upper molars of animals in all three groups generally reflected a significant loss of alveolar bone height, especially around the upper first molar. This bone loss was more accentuated at lower molars of group A than that of groups B and C, whereas at upper molars animals of all groups revealed similarly drastic bone loss buccally as well as interdentally. These differences between upper and lower molars cannot be explained at present. It is noteworthy, however, that the degree of bone loss in lower molars was unrelated to the individual antibody titers.

The stereological analysis of infiltrate composition was based on previously established methodology and examined at a limited sample size. Despite this limitation the congruence of infiltrate composition between buccal and interdental sites of both groups A and C animals was striking. In general, the results of this analysis corroborated histological observations which allowed a blind differentiation between groups A and C infiltrates. Although these data should be taken as relative rather than absolute figures, they illustrate a proportionally quite different constitution of infiltrate reactions in groups A and C animals.

At first sight, the large proportion of plasma cells in infiltrates of group A could be explained by the presence of sensitized precursors (memory cells) in central lymphoid tissues. These precursor cells having reached the local site would then be transformed into plasma cells in sequence to the peripheral presence of antigen. However, it has been shown by Humphrey and Turk (7), Kosunen and Flax (15), Leskowitz (17), and Flax et al. (2) that the preponderance

of plasma cells in peripheral infiltrates is by no means a characteristic of a distinct B-cell reaction. These authors have shown that cells of the plasma cell series dominate in late stages of local manifestations of delayed hypersensitivity reactions.

If this is true, intravenous sensitization had surely not exclusively resulted in a stimulation of the humoral immune system only but also in an activation of the cell-mediated immune system.

The infiltrates in group C, on the other hand, shared many traits of a delayed local hypersensitivity reaction and had in addition characteristics of a strong exudative phase which may be explained by chemotactic forces known to operate at the gingival margin (18). The intracutaneous sensitization had resulted in a significant but minor increase of serum antibodies. This points to the fact that the mode of sensitization of the animals in group C had also resulted in a weak activation of the antibody-mediated immune system. In spite of this fact, the infiltrates in group C were practically devoid of plasma cells, which in turn indicates that the continuous local antigenic stimulation is not answered by a rapid direct recruitment of presensitized B-cells from central lymphoid tissues. It appears furthermore that the group C type infiltrate represents an earlier stage than that observed in group A.

Although the present study reflects the composition of the infiltrated tissues at the terminal experimental stage only, the sequence of events may be reconstructed on the basis of the above-mentioned assumptions: (i) a pronounced acute exudative inflammatory phase as an initial response to the actinomyces plaque developing after inoculation; (ii) an infiltration of the peripheral connective and epithelial tissues by lymphocytes and development of a classic delayed hypersensitivity reaction in response to local sensitization or stimulation; (iii) maintenance of the delayed hypersensitivity reaction over prolonged periods of time because of the continuous antigenic challenge; and (iv) development of a superimposed plasma cell accumulation. All types of infiltrates observed in the present study can be classified according to these four phases. It is assumed that the animals of all groups experienced the phases (i) to (iii), possibly at different rates of progress, whereas phase (iv) was only reached in infiltrates of group A and in the interdental tissue of group B.

It is obvious that the connective tissue site harboring the densely packed infiltrates must have been directly affected by the invading cells. Regardless of the type of infiltrate (i.e.,

treatments A, B, and C) the collagen density within the infiltrated connective tissue was drastically reduced at interdental and buccal sites. In other words, all the infiltrated connective tissue areas contained less than 10% of the collagen density normally found in comparable gingival connective tissues of germfree rats (Schroeder and Jossi, unpublished data). Nevertheless, the number of fibroblasts observed per unit volume of infiltrated tissue in treatments B and C still ranged within the normal variability ($N_{vfi} 350 \times 10^6$ to $550 \times 10^6/cm^3$ of ICT). Plasma cell infiltrates of treatment A, however, revealed a reduced fibroblast density for buccal ($N_{vfi} 182 \times 10^6$) and for interdental sites ($N_{vfi} 257 \times 10^6$). In addition, the variably high proportion of residual tissue in infiltrates of all treatments and sites probably reflects an increased volume of proliferated blood vessels.

Our experimental data do not allow association of collagen loss with the activity of any cell type residing in the infiltrates, because it cannot be excluded that this breakdown had occurred already during the initial acute inflammatory phase. It is tempting to assume, however, that the pronounced fibroblast reduction occurring exclusively in treatment A is correlated with the superimposed plasma cell accumulation. If this is true, loss of a certain number of fibroblasts, carrying actinomyces antigens on their surface, by antibody-antigen complex-dependent cytotoxicity (4) or by complement-dependent lysis is very considerable.

In addition, the data collected allowed us to elaborate on the indirect relationship between infiltrates and bone remodeling. A most interesting and surprising finding of the present study is the observation that the degree of alveolar bone loss seems to be independent of the size and cellular composition of the infiltrated connective tissue fraction. Furthermore, the present data allowed us to postulate that the degree of bone loss observed was unrelated to the direct destructive capacity of the infiltrate as measured by the amount of collagen and number of fibroblasts remaining in the infiltrated connective tissue fraction. This strongly suggests the presence of distinct mechanisms responsible for the activation of osteoclasts on the one hand and factors interfering with fibroblast activity and collagen maintenance on the other. In other words, in order to induce a reduction of bone, the chronic pathological process does not have to contact bone surfaces directly.

In the present study, bone loss was apparently induced by a predominantly lymphoid infiltrate of a delayed hypersensitivity type with

or without superimposition of plasma cells. This is in contrast to a common observation in cases of human periodontitis in which bone loss seems to be consistently associated with extensive plasma cell infiltrates (9).

It is noteworthy that in the sham-immunized treatment B, only a predominantly lymphoid infiltrate occurred concomitantly with a plasma cell-rich infiltrate at different sites in the same animal. The observation that infiltrates of different character reside side by side and are locally confined in oral tissues of one particular subject is typically and consistently corroborated in man (33). One of the reasons for the plasma-rich infiltrate observed interdentally rather than buccally in treatment B seems to be the fact that hair impaction is more frequently and numerously experienced at this site. Impacted hairs can be observed to contain massive amounts of microorganisms, reach into the depths of gingival connective tissue, and probably act as an antigen-injecting syringe. It is only on these grounds that rapid tissue destruction in gnotobiotic, nonsensitized rats can be understood.

Hair impaction was equally frequent in all animals, i.e., in nonsensitized and sensitized rats. In spite of this fact, animals of group C exhibited exclusively an infiltrate typical for a delayed hypersensitivity reaction, whereas those of group A consistently revealed a plasma cell superimposition at all sites. This intriguing observation implies that the particular immune status (treatment C and A) was the significant factor determining the final type of peripheral infiltrative reaction. This statement, however, is based on quantitative cytology of the infiltrated connective tissue only. Unfortunately, no attempt was made to verify the presence of quantitative cell-mediated hypersensitivity by immunological procedures which would have allowed us to correlate the different types of infiltrates, tissue destruction, and bone loss to the degree of cell-mediated hypersensitivity. This important point must be considered in future studies.

ACKNOWLEDGMENTS

This investigation was supported by grants no. 3.278.69 and 3.312.70 from the Swiss National Foundation for the Advancement of Scientific Research.

LITERATURE CITED

- Costich, E. R. 1955. A quantitative evaluation of the effect of copper on alveolar bone loss in the syrian hamster. *J. Periodontol.* **26**:301-305.
- Flax, M. H., J. H. Elliott, J. J. Daly, K. Willms-Kretschmer, J. S. McCarthy, and S. Leskowitz. 1969. Local plasmacytopenesis in delayed hypersensitivity reactions. *J. Immunol.* **102**:1214-1219.
- Fraska, J. M., and V. R. Parks. 1965. A routine technique for double-staining ultrathin sections using uranyl and lead salts. *J. Cell. Biol.* **25**:157-161.
- Greenberg, A. H., and L. Shen. 1973. A class of specific cytotoxic cells demonstrated in vitro by arming with antigen-antibody complexes. *Nature N. Biol.* **245**:282-285.
- Hulin, Ch. 1929. L'état anaphylactique et la pyorrhée. *Odontologie* **67**:324-373.
- Hulin, Ch. 1931. Quelques idées personnelles sur la Pyorrhée alvéolaire. *Schweiz. Monatsschr. Zahnheilk.* **41**:931-962.
- Humphrey, J. H., and J. L. Turk. 1963. The effect of an unrelated delayed-type hypersensitivity reaction on the antibody response to diphtheria toxoid. *Immunology (London)* **6**:119-125.
- Hurni, H. 1968. Bauart und Betrieb eines Isolators. *Bibl. Microbiol.* **7**:54-58.
- James, W. W., and A. Counsell. 1927. A histological investigation into "so-called pyorrhoea alveolaris". *Brit. Dent. J.* **48**:1237-1253.
- Jordan, H. V., R. J. Fitzgerald, and H. R. Stanley. 1965. Plaque formation and periodontal pathology in gnotobiotic rats infected with an oral actinomycete. *Amer. J. Pathol.* **47**:1157-1167.
- Jordan, H. V., and P. H. Keyes. 1964. Aerobic, gram-positive, filamentous bacteria as etiologic agents of experimental periodontal disease in hamsters. *Arch. Oral Biol.* **9**:401-414.
- Jordan, H. V., and P. H. Keyes. 1965. Studies on the bacteriology of hamster periodontal disease. *Amer. J. Pathol.* **46**:843-857.
- Jordan, H. V., P. H. Keyes, and S. Bellack. 1972. Periodontal lesions in hamsters and gnotobiotic rats infected with actinomycetes of human origin. *J. Periodont. Res.* **7**:21-28.
- Keyes, P. H., and H. S. Gold. 1955. Periodontal lesions in the syrian hamster. I. A method of evaluating alveolar bone resorption. *Oral Surg. Oral Med. Oral Pathol.* **8**:492-499.
- Kosunen, T. U., and M. H. Flax. 1966. Experimental allergic thyroiditis in the guinea pig. IV. Autoradiographic studies of the evolution of the cellular infiltrate. *Lab. Invest.* **15**:606-616.
- Lehner, T. 1972. Cell-mediated immune responses in oral diseases: a review. *J. Oral Pathol.* **1**:39-58.
- Leskowitz, S. 1968. Is delayed sensitivity a preparation for antibody synthesis? *J. Immunol.* **101**:528-533.
- Lindhe, J., and L. Helldén. 1972. Neutrophilic chemotactic activity elaborated by human dental plaque. *J. Periodont. Res.* **7**:297-303.
- Luckey, T. D. 1963. *Germfree life and gnotobiology*, p. 494. Academic Press Inc., New York.
- Nisengard, R., E. H. Beutner, and S. P. Hazen. 1968. Immunologic studies of periodontal diseases. IV. Bacterial hypersensitivity and periodontal disease. *J. Periodont.* **39**:329-332.
- Ranney, R. R., and H. A. Zander. 1970. Allergic periodontal disease in sensitized squirrel monkeys. *J. Periodont.* **41**:12-21.
- Reynolds, E. S. 1963. The use of lead citrate at high pH as an electron opaque stain in electron microscopy. *J. Cell. Biol.* **17**:208-212.
- Rizzo, A. A., and C. T. Mitchell. 1966. Chronic allergic inflammation induced by repeated deposition of antigen in rabbit gingival pockets. *Periodontics* **4**:5-10.
- Schroeder, H. E. 1969. Ultrastructure of the junctional epithelium of the human gingiva. *Helv. Odont. Acta* **13**:65-83.
- Schroeder, H. E. 1973. Transmigration and infiltration of leucocytes in human junctional epithelium. *Helv. Odont. Acta* **17**:6-18.

26. Schroeder, H. E., J. Lindhe, A. Hugoson, and S. Münzel-Pedrazzoli. 1973. Structural constituents of clinically normal and slightly inflamed dog gingiva. A morphometric study. *Helv. Odont. Acta* 17:70-83.
27. Schroeder, H. E., and S. Münzel-Pedrazzoli. 1973. Correlated morphometric and biochemical analysis of gingival tissue: morphometric model, tissue sampling and test of stereotopic procedures. *J. Microsc.* 99:301-329.
28. Socransky, S. S., C. Hubersak, and D. Propas. 1970. Induction of periodontal destruction in gnotobiotic rats by a human oral strain of *Actinomyces naeslundii*. *Arch. Oral Biol.* 15:993-995.
29. Takatsy, G. 1955. The use of spiral loops in serological and virological micro-methods. *Acta Microbiol. Hung.* 3:191-202.
30. Terner, C. 1965. Arthus reaction in the oral cavity of laboratory animals. *Periodontics* 3:18-22.
31. Weibel, E. R. 1969. Stereological principles for morphometry electron microscopic cytology. *Int. Rev. Cytol.* 26:235-302.
32. Weibel, E. R. 1970. An automatic sampling stage microscope for stereology. *J. Microsc.* 91:1-18.
33. Zachrisson, B. M., and S. D. Schultz-Hautd. 1968. A comparative histotopical study of clinically normal and chronically inflamed gingivae from the same individuals. *Odont. Tidskr.* 76:179-192.